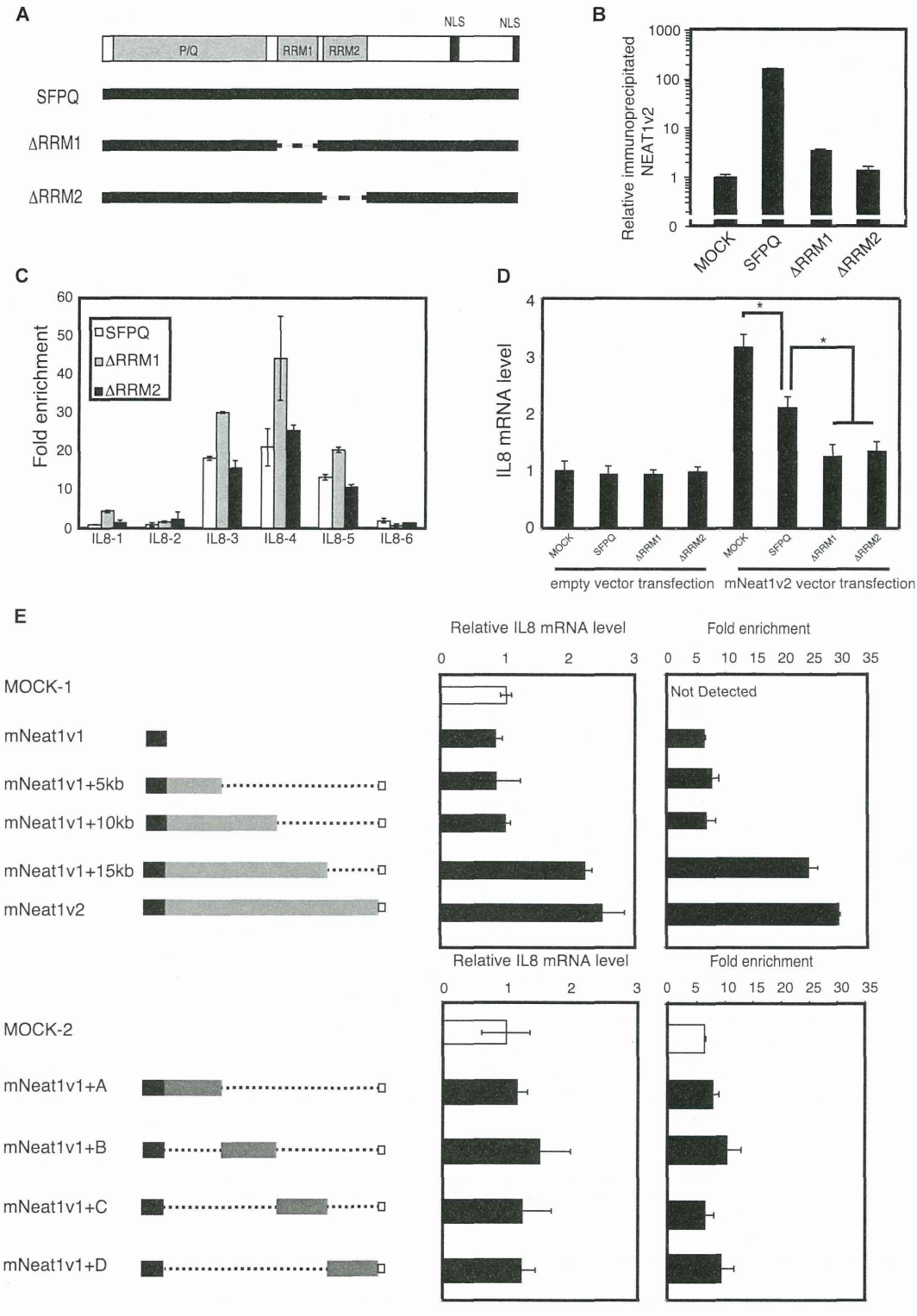

(legend on next page)

cells (Figure 5G). These results indicate that NEAT1 is induced by certain viruses and that it plays an important role in the innate immune response to viral infection.

DISCUSSION

In this study, we report that NEAT1 is induced by viral infection as well as by poly I:C stimulation. Moreover, we found that the stimulus-responsive cooperative action of NEAT1 and SFPQ regulates the expression of genes including those of antiviral factors such as cytokines (Figure 6).

The mechanisms of action of lncRNAs are diverse, ranging from guidance of the chromatin-modifying complexes to acting as "molecular sponges" for the capture of microRNAs (Mercer et al., 2009; Wang and Chang, 2011). For example, lncRNA GAS5 interacts directly with the DNA-binding domain of the glucocorticoid receptor, preventing the receptor from binding to its DNA response element, thereby in effect acting as a molecular decoy (Kino et al., 2010; Tani et al., 2013). LncRNA MALAT1 and TUG1 promote the relocalization of growth-control genes between nuclear subcompartments and thereby regulate gene expression during growth signaling (Yang et al., 2011). More recently, Hirose et al. reported the role of NEAT1 in transcriptional regulation through the sequestering of SFPQ from the RNA-specific adenosine deaminase B2 (ADARB2) gene in response to proteasome inhibition (Hirose et al., 2014). In contrast to our result, the authors showed the importance of the NEAT1-SFPQ interaction in the reduction of ADARB2 transcription. Thus, the NEAT1-SFPQ interaction plays roles in both repression and activation of genes, likely depending on the context of the promoter sequence or interplay with other transcriptional factor(s).

Although there are increasing data that show that lncRNA-protein interactions appear to function in the regulation of gene expression patterns, the identification of the critical short RNA sequences in functional lncRNAs was limited. We attempted to determine the minimal short RNA region in NEAT1 with which SFPQ interacts. We extrapolated the SFPQ binding region in NEAT1v2 by employing the data set of a recent study that systematically identified the RNA sequence motifs recognized by SFPQ (Ray et al., 2013). The potential SFPQ binding sequences were identified in a broad region of NEAT1v2 (Figure S4A). Among these potential SFPQ binding sequences, we showed that two NEAT1 sequences, containing highly ranked SFPQ-binding RNA sequences reported by Ray et al., bound directly and specifically to SFPQ (Figures S4B–S4D). These SFPQ-binding NEAT1 RNAs did not affect the level of mNeat1v2-mediated IL8 transcription (Figure S4E), corresponding to the result in Figure 4. It has been reported that certain RNA binding proteins require a long length of the RNA binding partner to achieve adequate protein function. For instance, polycomb repressive complex 2 (PRC2), containing an RNA binding protein, shows higher affinity to longer partner lncRNAs (Davidovich et al., 2013). In a similar manner as PRC2, SFPQ may require a long NEAT1 RNA sequence (~15 kb) to exert proper function, namely releasing from the IL8 promoter as described in this research.

In this report, we focused on the role of NEAT1 in host antiviral response. However, NEAT1 is also likely to regulate the expression of viral genes themselves, because several paraspeckle proteins are known to play a role in viral replication or viral gene expression (Oakland et al., 2013; Zhang et al., 2008; Zolotukhin et al., 2003). It is reasonable to assume that NEAT1-mediated remodeling of the nuclear localization of paraspeckle proteins directly affects viral replication and/or viral gene expression. Indeed, a recent report observed that NEAT1 modulates HIV-I replication by affecting the nucleus-to-cytoplasm export of Rev-dependent instability element-containing HIV-I mRNAs (Zhang et al., 2013). They showed that MALAT1 lncRNA localized in nuclear speckles was also induced by HIV infection. However, MALAT1 was not induced by poly I:C treatment and virus infections (Figure S5I). Thus, the induction of NEAT1 in response to viral infection may be a more general phenomenon than MALAT1 induction. In the present work, we propose that the TLR3-p38 pathway contributes to the induction of NEAT1 in response to poly I:C stimulation. Since poly I:C generally simulates the action of dsRNAs produced by viral infection, we speculate that viral infections also induce NEAT1 through the TLR3-p38 pathway. Analysis of the paraspeckle entities will reveal a novel mode(s) of viral replication and will contribute to a deeper understanding of viral life cycles and to the development of antiviral drugs.

The transcriptional regulation of cytokine genes in response to pathogen infection lies at the heart of immune response research. In terms of the transcriptional activation of the *IL8* gene, NF-κB, AP-1, and C/EBP play an important role. In this report, we have added another layer to knowledge of the transcriptional regulation system by uncovering the cooperative action between nuclear lncRNA and transcriptional regulator. The

Figure 4. Structure-Function Relationship Study of SFPQ and NEAT1

(A) Schematic diagrams of SFPQ deletion mutants. P/Q, RRM, and NLS indicate the P/Q domain, RNA binding motif, and nuclear localization signal, respectively. Dashed lines indicate the deleted regions in the mutant SFPQs.

(B) RNA immunoprecipitation experiment of the SFPQs. Cells transfected with plasmids expressing FLAG-tagged SFPQs were subjected to immunoprecipitation using an anti-FLAG antibody (clone M2; Sigma). The amounts of NEAT1v2 coimmunoprecipitated with the indicated FLAG-tagged SFPQs were determined by RT-qPCR analysis. The relative amounts of NEAT1v2 isolated by the anti-FLAG antibody were normalized to that isolated by the control IgG.

(C) ChIP analysis of the 5′ region of the *IL8* gene in HeLa TO cells transfected with plasmids expressing the indicated FLAG-tagged SFPQs. The relative amounts of IL8 promoter region DNA isolated by the anti-FLAG antibody were normalized to that isolated by the control IgG. Error bars indicate the errors of two replicate experiments.

(D) IL8 mRNA levels in HeLa TO cells transfected with plasmids expressing the indicated SFPQs in the presence or absence of mNeat1v2 expression. Values represent the mean ± SD (*$p < 0.01$, Student's t test).

(E) IL8 mRNA induction activity and SFPQ binding activity of mutant mNeat1s. Black and gray boxes indicate mNeat1v1 and mNeat1v2, respectively. Dashed lines indicate deleted regions. Schematic structures of the mNeat1v2 deletion mutants are indicated on the left. IL8 mRNA induction determined by RT-qPCR and SFPQ binding determined by RNA immunoprecipitation experiments are shown in the center and right, respectively.

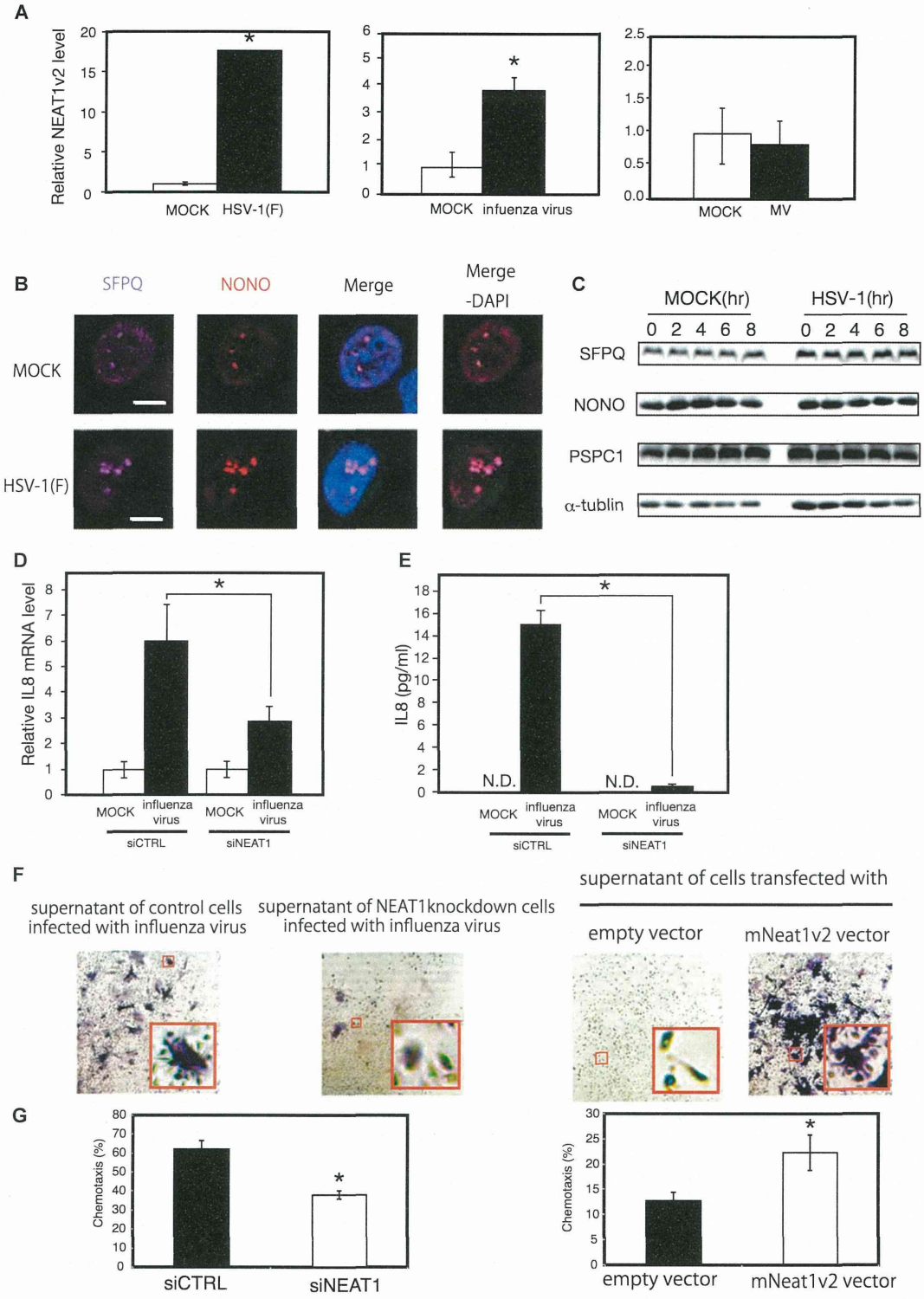

Figure 5. Effect of Viral Infection on NEAT1v2 Induction, Paraspeckle Formation, IL8 Induction, and the Activation of Bone Marrow Cells

(A) NEAT1v2 levels were quantified by RT-qPCR in cells infected with influenza virus, herpes simplex virus 1 (HSV-1), or measles virus (MV). The 18S ribosomal RNA level was used as a normalization control. Values represent the mean ± SD (*$p < 0.01$, Student's t test).

(legend continued on next page)

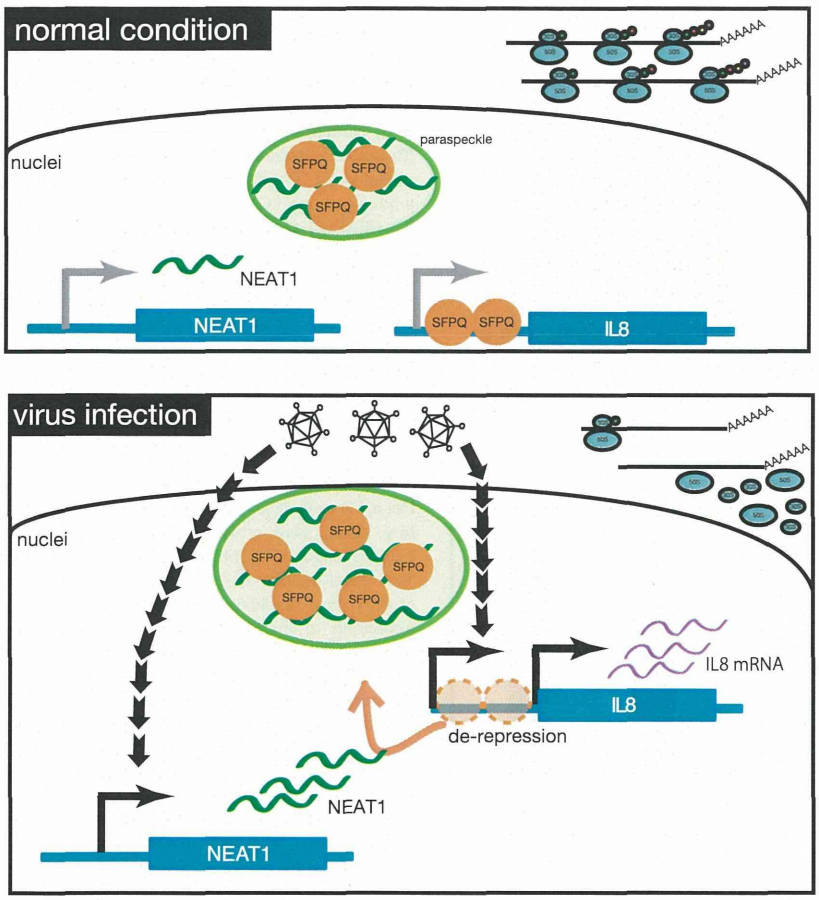

Figure 6. Model of the Transcriptional Regulation of Antiviral Genes Regulated by the Coordinated Action of NEAT1 and Paraspeckle Protein

SFPQs are both located in paraspeckles and bound to gene promoters such as *IL8* under normal conditions. Here, SFPQ represses the transcription of the *IL8* gene. Upon viral infection or poly I:C stimulation, NEAT1 is induced. In the case of poly I:C stimulation, NEAT1 is induced by the TLR3-p38 pathway. NEAT1 induction relocates SFPQ from the *IL8* promoter region and forms excess paraspeckles, consequently activating *IL8* transcription.

high evolutionary conservation of the SFPQ-binding sequence (Figure 3C and Table S3), comparable to that of the AP-1 and C/EBP sites, emphasizes the importance of SFPQ-mediated transcriptional regulation of the *IL8* gene. The established modes of transcriptional activation (NF-κB and so on) and the lncRNA-mediated mode of transcriptional regulation (this study) therefore work in synergy to achieve the precise transcriptional regulation of cytokine genes required during immune response.

SFPQ is known as a multifunctional protein involved in several vital cellular processes, such as pre-mRNA processing. We therefore examined whether NEAT1 controls the function of SFPQ in splicing. We surveyed genes whose splicing patterns were influenced by poly I:C treatment and restored by NEAT1 depletion through a massive sequencing analysis. The poly I:C-induced altered splicing of the *Serine palmitoyltransferase, long chain base subunit 1* gene (increase in variant NM_178324 from 20% to 33%) was restored by NEAT1 depletion (from 28% to 33%) (Figures S2J and S2K). Thus, NEAT1 is also involved in the regulation of SFPQ-mediated splicing regulation.

In this report, there are somewhat superficial nonlinear correlations among NEAT1 expression level, IL8 expression level, SFPQ localization, and paraspeckle size. We think that these superficial nonlinear correlations can be explained by the following interpretations. The *IL8* transcription is regulated by not only NEAT1-SFPQ cooperation, but also the NF-κB pathway. Since both poly I:C treatment and virus infection activate the NF-κB pathway, the effects of these stimuli for IL8 transcription are stronger than that of NEAT1 overexpression, which can only activate SFPQ-mediated IL8 transcription. Therefore, the elevated level of NEAT1v2 (causing excess formation of paraspeckles, but not inducing NF-κB activation) did not lead to a strong induction of IL8 mRNA expression compared with poly I:C treatment or viral infections. Another potential explanation is the presence of multiple functions in SFPQ. Several SFPQ-mediated gene regulation pathways might be involved in the upregulation of IL8 mRNA expression in response to SFPQ depletion. If SFPQ destabilized IL8 mRNA, depletion of SFPQ would increase IL8 mRNA through mRNA stabilization and transcriptional activation. If this was the

(B) HeLa TO cells infected with HSV-1 were subjected to visualization of SFPQ (magenta) and NONO (red) by immunostaining, and of the nuclei by staining with DAPI.
(C) The levels of paraspeckle proteins were analyzed by western blotting at various points post-HSV-1 infection.
(D and E) IL8 mRNA and protein levels were quantified by RT-qPCR and ELISA, respectively, in NEAT1 knockdown cells or control cells infected with (black bars) or without (white bars) influenza virus. Values represent the mean ± SD (*$p < 0.01$, Student's t test).
(F) Microscopic observation of mouse bone marrow cells treated with the supernatants of the indicated cultured cells. The cells were stained using a TRACP and ALP double-stain kit. The red color-stained cells show TRACP activity, indicating the osteoclast differentiation. The blue color-stained cells show ALP activity, indicating the osteoblast differentiation. Values represent the mean ± SD (*$p < 0.01$, Student's t test).
(G) Chemotaxis of DMSO-HL60 cells were assessed by transwell assay. Migrated cells were counted under microscopic observation. Chemotaxis values ((migrated cells / total cells) × 100) represent the means ± SD of three independent experiments. Statistically significant differences ($p < 0.01$) were determined by Student's t test.

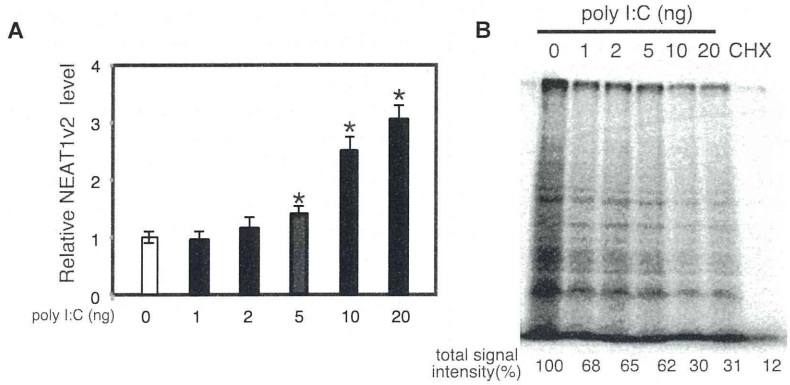

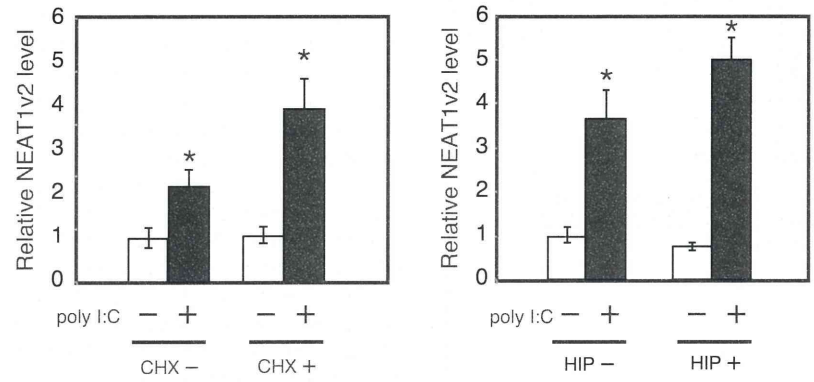

Figure 7. Induction of NEAT1v2 by Poly I:C under Translational Repression

(A) NEAT1v2 levels in cells transfected with the indicated amounts of poly I:C were quantified by RT-qPCR. Values represent the mean ± SD (*$p < 0.01$, Student's t test).

(B) Global translation status of transcription-incompetent HeLa TO cells transfected with the indicated amounts of poly I:C.

(C) NEAT1v2 levels were quantified by RT-qPCR in cells transfected with or without poly I:C under either cycloheximide (CHX; inhibitor for translational elongation) or hippuristanol (HIP; inhibitor for translational initiation) treatments. Values represent the mean ± SD (*$p < 0.01$, Student's t test).

case, depletion of SFPQ would have a stronger effect on the level of IL8 mRNA expression compared with NEAT1 induction-mediated SFPQ modulation. In addition, although NEAT1 should relocate SFPQ from the IL8 promoter, SFPQ proteins are still present in the nucleus. Such SFPQ, even enriched in paraspeckles, might have a certain effect on the IL8 mRNA expression level.

Translation in virus-infected cells is highly repressed (Sonenberg, 1990). For this reason, a translation-independent acute response system is necessary for early immune response. In this regard, the system proposed here is biologically meaningful, because NEAT1 is a noncoding RNA that exerts an effect without need for translation. Indeed, NEAT1 was induced in cells where translation was repressed by poly I:C stimulation (Figure 7). NEAT1v2 was also induced in cells treated with specific translation inhibitors (Figure 7). Translational inhibition did not affect the amounts of paraspeckle proteins (Figure S6B) or the formation of paraspeckles (Figure S6A). These results show that NEAT1v2 exerts an effect under translational repression. We therefore speculate that many other lncRNAs play a role in situations where translation is highly repressed, such as viral infection, heat shock, and hypoxia.

EXPERIMENTAL PROCEDURES

Reagents and Molecular Biological Products

All chemicals were purchased from Wako, unless otherwise stated.

Cell Culture and Transfection

HeLa TO cells (Clontech) and A549 cells (laboratory stock) were grown in Dulbecco's modified Eagle's medium (DMEM), supplemented with 10% fetal bovine serum (FBS) and antibiotics at 37°C in a humidified incubator with 5% CO_2. According to the manufacturer's protocol, cells were transfected with poly I:C or plasmid DNA using Lipofectamine 2000 or Lipofectamine LTX (Invitrogen), respectively. For poly I:C stimulation, cells were seeded into 12-well cell culture plates followed by transfection using the indicated amounts of poly I:C and Lipofectamine 2000. The sequences of the siRNAs are listed in Table S2. siRNAs were transfected into cells using Lipofectamine RNAiMAX (Invitrogen) according to the manufacturer's instructions. Briefly, siRNA duplexes (final concentration 10 nM) and cells were harvested 72 hr posttransfection. RT-qPCR was used to determine whether RNA interference achieved significant depletion of each target sequence.

ChIP Assay

Chromatin was crosslinked with 1% formaldehyde for 10 min at 37°C and then sonicated in lysis buffer (1% SDS, 10 mM EDTA, and 50 mM Tris [pH 8.0], plus protease inhibitor cocktail [Roche]). After centrifugation, 10 μl of the supernatant was used as input, and the remaining lysate was subjected to a ChIP assay using an anti-SFPQ mouse monoclonal antibody (clone B92, Sigma-Aldrich). The primers used to amplify the genes are listed in Table S1.

Viral Infection

HeLa TO cells were seeded into culture plates 1 day before infection and then infected with HSV-1(F) at a multiplicity of infection (moi) of 10. At 72 hr posttransfection with either siRNA or *mNeat1* cDNA, HeLa cells grown in DMEM supplemented with 10% FCS were infected with influenza A virus strain A/WSN/33 at a moi of 3. After incubation for 15 hr, the culture supernatants and total RNAs were collected and subjected to ELISA and RT-qPCR, respectively. MV (Edmonston strain) was propagated in Vero cells grown in DMEM supplemented with 2% FCS. A549 cells were infected with MV at a moi of 0.1.

SUPPLEMENTAL INFORMATION

Supplemental Information includes six figures, four tables, Supplemental Experimental Procedures, and two movies and can be found with this article online at http://dx.doi.org/10.1016/j.molcel.2014.01.009.

AUTHOR CONTRIBUTIONS

K.I., K.S., and N.A. conceived the research strategies, performed experiments, and wrote the paper. N.I., T. Yada, and Y.S. performed bioinformatics analyses. G.A. performed FISH and IF. T. Yamada and T.O. performed FRAP analysis and wrote the manuscript. M. Kumakura, A. Kawaguchi, K.N., A. Kato, Y.K., H.S., M.Y., and C.K. designed the virus infection experiments, performed experiments, and wrote the manuscript. T. Yada analyzed the SFPQ binding region and wrote the paper. K.K., K.I., M. Kobayashi, T.K., and Y.W. designed the microarray analysis, performed experiments, and wrote the manuscript.

ACKNOWLEDGMENTS

We thank Drs. T. Hirose (Hokkaido University) and S. Nakagawa (Riken) for providing mouse Neat1 expression vectors. We thank Drs. Y. Tomari (University of Tokyo), Y. Kumagai (Osaka University), Y.T. Sasaki (AIST), and Y. Hayashi (University of Tokyo) for fruitful discussion and critical comments. We also thank Dr. A. Fox (University of Western Australia), K. Lynch (University of Pennsylvania), A. Matsuzawa (University of Tokyo), and Y. Yoneyama (Chiba University) for providing the mouse monoclonal anti-NONO/p54 antibody, the HIS-SFPQ expression vector, anti-phospho-JNK antibody, and shRNA expression vector to silence RIG-I, respectively. This work was financially supported by the Suzuken Memorial Foundation, the Naito Foundation, Research Fellowship of the Japan Society for the Promotion of Science, Grant-in-Aid for Scientific Research (22310117, 23659050, 23790077), a Grant-in-Aid for Scientific Research on Innovative Areas "Functional machinery for noncoding RNAs," "Genome adaptation," and "Genome science" from the Ministry of Education, Culture, Sports, Science and Technology of Japan, and The Funding Program for World-Leading Innovative R&D on Science and Technology of the Japan Society for the Promotion of Science.

Received: June 6, 2013
Revised: November 8, 2013
Accepted: January 2, 2014
Published: February 6, 2014

REFERENCES

Arpaia, N., and Barton, G.M. (2011). Toll-like receptors: key players in antiviral immunity. Curr Opin Virol *1*, 447–454.

Berghäll, H., Sirén, J., Sarkar, D., Julkunen, I., Fisher, P.B., Vainionpää, R., and Matikainen, S. (2006). The interferon-inducible RNA helicase, mda-5, is involved in measles virus-induced expression of antiviral cytokines. Microbes Infect. *8*, 2138–2144.

Bernard, D., Prasanth, K.V., Tripathi, V., Colasse, S., Nakamura, T., Xuan, Z., Zhang, M.Q., Sedel, F., Jourdren, L., Coulpier, F., et al. (2010). A long nuclear-retained non-coding RNA regulates synaptogenesis by modulating gene expression. EMBO J. *29*, 3082–3093.

Carninci, P., Kasukawa, T., Katayama, S., Gough, J., Frith, M.C., Maeda, N., Oyama, R., Ravasi, T., Lenhard, B., Wells, C., et al.; FANTOM Consortium; RIKEN Genome Exploration Research Group and Genome Science Group (Genome Network Project Core Group) (2005). The transcriptional landscape of the mammalian genome. Science *309*, 1559–1563.

Chen, L.L., and Carmichael, G.G. (2009). Altered nuclear retention of mRNAs containing inverted repeats in human embryonic stem cells: functional role of a nuclear noncoding RNA. Mol. Cell *35*, 467–478.

Chen, L.L., and Carmichael, G.G. (2010). Decoding the function of nuclear long non-coding RNAs. Curr. Opin. Cell Biol. *22*, 357–364.

Clemson, C.M., Hutchinson, J.N., Sara, S.A., Ensminger, A.W., Fox, A.H., Chess, A., and Lawrence, J.B. (2009). An architectural role for a nuclear noncoding RNA: NEAT1 RNA is essential for the structure of paraspeckles. Mol. Cell *33*, 717–726.

Davidovich, C., Zheng, L., Goodrich, K.J., and Cech, T.R. (2013). Promiscuous RNA binding by Polycomb repressive complex 2. Nat. Struct. Mol. Biol. *20*, 1250–1257.

Fox, A.H., and Lamond, A.I. (2010). Paraspeckles. Cold Spring Harb. Perspect. Biol. *2*, a000687.

Guillot, L., Le Goffic, R., Bloch, S., Escriou, N., Akira, S., Chignard, M., and Si-Tahar, M. (2005). Involvement of toll-like receptor 3 in the immune response of lung epithelial cells to double-stranded RNA and influenza A virus. J. Biol. Chem. *280*, 5571–5580.

Gupta, R.A., Shah, N., Wang, K.C., Kim, J., Horlings, H.M., Wong, D.J., Tsai, M.C., Hung, T., Argani, P., Rinn, J.L., et al. (2010). Long non-coding RNA HOTAIR reprograms chromatin state to promote cancer metastasis. Nature *464*, 1071–1076.

Guttman, M., Amit, I., Garber, M., French, C., Lin, M.F., Feldser, D., Huarte, M., Zuk, O., Carey, B.W., Cassady, J.P., et al. (2009). Chromatin signature reveals over a thousand highly conserved large non-coding RNAs in mammals. Nature *458*, 223–227.

Hirose, T., Virnicchi, G., Tanigawa, A., Naganuma, T., Li, R., Kimura, H., Yokoi, T., Nakagawa, S., Bénard, M., Fox, A.H., and Pierron, G. (2014). NEAT1 long noncoding RNA regulates transcription via protein sequestration within subnuclear bodies. Mol. Biol. Cell *25*, 169–183.

Hoffmann, E., Dittrich-Breiholz, O., Holtmann, H., and Kracht, M. (2002). Multiple control of interleukin-8 gene expression. J. Leukoc. Biol. *72*, 847–855.

Huarte, M., and Rinn, J.L. (2010). Large non-coding RNAs: missing links in cancer? Hum. Mol. Genet. *19* (R2), R152–R161.

Hutchinson, J.N., Ensminger, A.W., Clemson, C.M., Lynch, C.R., Lawrence, J.B., and Chess, A. (2007). A screen for nuclear transcripts identifies two linked noncoding RNAs associated with SC35 splicing domains. BMC Genomics *8*, 39.

Iacobazzi, V., Infantino, V., Costanzo, P., Izzo, P., and Palmieri, F. (2005). Functional analysis of the promoter of the mitochondrial phosphate carrier human gene: identification of activator and repressor elements and their transcription factors. Biochem. J. *391*, 613–621.

Kapranov, P., Willingham, A.T., and Gingeras, T.R. (2007). Genome-wide transcription and the implications for genomic organization. Nat. Rev. Genet. *8*, 413–423.

Kawai, T., and Akira, S. (2010). The role of pattern-recognition receptors in innate immunity: update on Toll-like receptors. Nat. Immunol. *11*, 373–384.

Kino, T., Hurt, D.E., Ichijo, T., Nader, N., and Chrousos, G.P. (2010). Noncoding RNA gas5 is a growth arrest- and starvation-associated repressor of the glucocorticoid receptor. Sci. Signal. *3*, ra8.

Koide, M., Kinugawa, S., Takahashi, N., and Udagawa, N. (2010). Osteoclastic bone resorption induced by innate immune responses. Periodontol. 2000 *54*, 235–246.

Lafaille, F.G., Pessach, I.M., Zhang, S.Y., Ciancanelli, M.J., Herman, M., Abhyankar, A., Ying, S.W., Keros, S., Goldstein, P.A., Mostoslavsky, G., et al. (2012). Impaired intrinsic immunity to HSV-1 in human iPSC-derived TLR3-deficient CNS cells. Nature *491*, 769–773.

Mao, Y.S., Zhang, B., and Spector, D.L. (2011). Biogenesis and function of nuclear bodies. Trends Genet. *27*, 295–306.

Mercer, T.R., Dinger, M.E., and Mattick, J.S. (2009). Long non-coding RNAs: insights into functions. Nat. Rev. Genet. *10*, 155–159.

Miyagawa, R., Tano, K., Mizuno, R., Nakamura, Y., Ijiri, K., Rakwal, R., Shibato, J., Masuo, Y., Mayeda, A., Hirose, T., and Akimitsu, N. (2012). Identification of cis- and trans-acting factors involved in the localization of MALAT-1 noncoding RNA to nuclear speckles. RNA *18*, 738–751.

Mizutani, R., Wakamatsu, A., Tanaka, N., Yoshida, H., Tochigi, N., Suzuki, Y., Oonishi, T., Tani, H., Tano, K., Ijiri, K., et al. (2012). Identification and characterization of novel genotoxic stress-inducible nuclear long noncoding RNAs in mammalian cells. PLoS ONE *7*, e34949.

Naganuma, T., and Hirose, T. (2013). Paraspeckle formation during the biogenesis of long non-coding RNAs. RNA Biol. *10*, 456–461.

Naganuma, T., Nakagawa, S., Tanigawa, A., Sasaki, Y.F., Goshima, N., and Hirose, T. (2012). Alternative 3′-end processing of long noncoding RNA initiates construction of nuclear paraspeckles. EMBO J. *31*, 4020–4034.

Nakagawa, S., and Hirose, T. (2012). Paraspeckle nuclear bodies—useful uselessness? Cell. Mol. Life Sci. *69*, 3027–3036.

Oakland, T.E., Haselton, K.J., and Randall, G. (2013). EWSR1 binds the hepatitis C virus cis-acting replication element and is required for efficient viral replication. J. Virol. *87*, 6625–6634.

Peng, R., Dye, B.T., Pérez, I., Barnard, D.C., Thompson, A.B., and Patton, J.G. (2002). PSF and p54nrb bind a conserved stem in U5 snRNA. RNA *8*, 1334–1347.

Ponting, C.P., Oliver, P.L., and Reik, W. (2009). Evolution and functions of long noncoding RNAs. Cell *136*, 629–641.

Prasanth, K.V., and Spector, D.L. (2007). Eukaryotic regulatory RNAs: an answer to the 'genome complexity' conundrum. Genes Dev. *21*, 11–42.

Rathinam, V.A., and Fitzgerald, K.A. (2011). Cytosolic surveillance and antiviral immunity. Curr Opin Virol *1*, 455–462.

Ray, D., Kazan, H., Cook, K.B., Weirauch, M.T., Najafabadi, H.S., Li, X., Gueroussov, S., Albu, M., Zheng, H., Yang, A., et al. (2013). A compendium of RNA-binding motifs for decoding gene regulation. Nature *499*, 172–177.

Saha, S., Murthy, S., and Rangarajan, P.N. (2006). Identification and characterization of a virus-inducible non-coding RNA in mouse brain. J. Gen. Virol. *87*, 1991–1995.

Sasaki, Y.T., Ideue, T., Sano, M., Mituyama, T., and Hirose, T. (2009). MENepsilon/beta noncoding RNAs are essential for structural integrity of nuclear paraspeckles. Proc. Natl. Acad. Sci. USA *106*, 2525–2530.

Scaria, V., and Pasha, A. (2012). Long Non-Coding RNAs in Infection Biology. Front Genet *3*, 308.

Sonenberg, N. (1990). Measures and countermeasures in the modulation of initiation factor activities by viruses. New Biol. *2*, 402–409.

Song, X., Sui, A., and Garen, A. (2004). Binding of mouse VL30 retrotransposon RNA to PSF protein induces genes repressed by PSF: effects on steroidogenesis and oncogenesis. Proc. Natl. Acad. Sci. USA *101*, 621–626.

Sunwoo, H., Dinger, M.E., Wilusz, J.E., Amaral, P.P., Mattick, J.S., and Spector, D.L. (2009). MEN epsilon/beta nuclear-retained non-coding RNAs are up-regulated upon muscle differentiation and are essential components of paraspeckles. Genome Res. *19*, 347–359.

Tani, H., Mizutani, R., Salam, K.A., Tano, K., Ijiri, K., Wakamatsu, A., Isogai, T., Suzuki, Y., and Akimitsu, N. (2012). Genome-wide determination of RNA stability reveals hundreds of short-lived noncoding transcripts in mammals. Genome Res. *22*, 947–956.

Tani, H., Torimura, M., and Akimitsu, N. (2013). The RNA degradation pathway regulates the function of GAS5 a non-coding RNA in mammalian cells. PLoS ONE *8*, e55684.

Tano, K., Mizuno, R., Okada, T., Rakwal, R., Shibato, J., Masuo, Y., Ijiri, K., and Akimitsu, N. (2010). MALAT-1 enhances cell motility of lung adenocarcinoma cells by influencing the expression of motility-related genes. FEBS Lett. *584*, 4575–4580.

Thompson, M.R., Kaminski, J.J., Kurt-Jones, E.A., and Fitzgerald, K.A. (2011). Pattern recognition receptors and the innate immune response to viral infection. Viruses *3*, 920–940.

Urban, R.J., Bodenburg, Y., Kurosky, A., Wood, T.G., and Gasic, S. (2000). Polypyrimidine tract-binding protein-associated splicing factor is a negative regulator of transcriptional activity of the porcine p450scc insulin-like growth factor response element. Mol. Endocrinol. *14*, 774–782.

Wang, K.C., and Chang, H.Y. (2011). Molecular mechanisms of long noncoding RNAs. Mol. Cell *43*, 904–914.

Yang, L., Lin, C., Liu, W., Zhang, J., Ohgi, K.A., Grinstein, J.D., Dorrestein, P.C., and Rosenfeld, M.G. (2011). ncRNA- and Pc2 methylation-dependent gene relocation between nuclear structures mediates gene activation programs. Cell *147*, 773–788.

Yoon, J.H., Abdelmohsen, K., and Gorospe, M. (2013). Posttranscriptional Gene Regulation by Long Noncoding RNA. J. Mol. Biol. *425*, 3723–3730.

Zhang, S.Y., Jouanguy, E., Ugolini, S., Smahi, A., Elain, G., Romero, P., Segal, D., Sancho-Shimizu, V., Lorenzo, L., Puel, A., et al. (2007). TLR3 deficiency in patients with herpes simplex encephalitis. Science *317*, 1522–1527.

Zhang, W., Zhang, X., Tian, C., Wang, T., Sarkis, P.T., Fang, Y., Zheng, S., Yu, X.F., and Xu, R. (2008). Cytidine deaminase APOBEC3B interacts with heterogeneous nuclear ribonucleoprotein K and suppresses hepatitis B virus expression. Cell. Microbiol. *10*, 112–121.

Zhang, Q., Chen, C.Y., Yedavalli, V.S., and Jeang, K.T. (2013). NEAT1 long noncoding RNA and paraspeckle bodies modulate HIV-1 posttranscriptional expression. MBio *4*, e00596–e12.

Zolotukhin, A.S., Michalowski, D., Bear, J., Smulevitch, S.V., Traish, A.M., Peng, R., Patton, J., Shatsky, I.N., and Felber, B.K. (2003). PSF acts through the human immunodeficiency virus type 1 mRNA instability elements to regulate virus expression. Mol. Cell. Biol. *23*, 6618–6630.

Biochemical and Biophysical Research Communications 443 (2014) 975–979

Contents lists available at ScienceDirect

Biochemical and Biophysical Research Communications

journal homepage: www.elsevier.com/locate/ybbrc

Involvement of the N-terminal portion of influenza virus RNA polymerase subunit PB1 in nucleotide recognition

Nguyen Trong Binh [b], Chitose Wakai [a], Atsushi Kawaguchi [a,b], Kyosuke Nagata [c,*]

[a] Department of Infection Biology, Faculty of Medicine, University of Tsukuba, 1-1-1 Tennodai, Tsukuba 305-8575, Japan
[b] Graduate School of Comprehensive Human Sciences, University of Tsukuba, 1-1-1 Tennodai, Tsukuba 305-8575, Japan
[c] University of Tsukuba, 1-1-1 Tennodai, Tsukuba 305-8575, Japan

ARTICLE INFO

Article history:
Received 26 November 2013
Available online 19 December 2013

Keywords:
Influenza
Nucleotide recognition
Resistant mutant
Ribavirin

ABSTRACT

The influenza virus PB1 protein functions as a catalytic subunit of the viral RNA-dependent RNA polymerase and contains the highly conserved motifs of RNA-dependent RNA polymerases together with putative nucleotide-binding sites. PB1 also binds to viral genomic RNAs and its replicative intermediates through the promoter regions. The detail function and interplay between functional domains are not clarified although a part of structures and functions of PB1 have been clarified. In this study, we analyzed the function of PB1 subunit in the sense of nucleotide recognition using ribavirin, which is a nucleoside analog and inhibits viral RNA synthesis of many RNA viruses including influenza virus. We screened ribavirin-resistant PB1 mutants from randomly mutated PB1 cDNA library using a mini-replicon assay, and we identified a single mutation at the amino acid position 27 of PB1 as an important residue for the nucleotide recognition.

1. Introduction

Influenza A virus belongs to the family of *Orthomyxoviridae*. Its genome consists of eight-segmented and single-stranded RNAs of negative polarity (vRNA). Each segment is encapsidated by nucleoprotein (NP) and associated with viral RNA polymerases to form viral ribonucleoprotein (vRNP) complexes. The vRNP complex is a basic unit for both transcription and replication [1]. The viral mRNA transcription is initiated using capped oligonucleotide as a primer. The elongation of mRNA chain proceeds until the viral polymerase reaches oligo U sequence present near the 5′-terminus of vRNA, and then the poly A tail is added by the viral RNA polymerase. In the viral genome replication, full-length cRNA (complementary RNA to vRNA) is generated from vRNA in a primer-independent manner, and progeny vRNAs are amplified from cRNA by the viral RNA polymerase. The viral RNA polymerase consists of PB1, PB2, and PA. PB1 functions as a catalytic subunit and the assembly core of the viral RNA polymerase [2–7]. PA is genetically found to be involved in the replication process and the polymerase assembly [8] and have the endonuclease activity [9–12]. PB2 is responsible for the recognition and binding of the cap structure [1,13–16].

The 14 amino acids residues from the N-terminus of PB1 interact with PA [4–7,17–20], while the C-terminal region of PB1 between amino acid (a.a.) positions 678–757 interacts with PB2 [4–6,21,22]. PB1 contains the motifs highly conserved among RNA-dependent RNA polymerases [2]. There are two putative nucleotide-binding sites between a.a. positions 179–297 and 458–519 [23,24]. Moreover, the N-terminal (a.a. positions 1–83) and C-terminal (a.a. positions 494–757) regions of PB1 are suggested to interact with the vRNA promoter [25]. In addition, the a.a. positions 249–254 of PB1 is important for the vRNA binding, and Phe251 (when the number indicates the amino acid position) and Phe254 are essential for this binding [26]. It is also reported that the regions between a.a. positions 1–139 and 267–493 bind to the cRNA promoter [27].

Ribavirin (1-β-D-ribofusanosyl-1,2,4-triazole-3-carboxamide, also known as Virazole) is a synthetic purine nucleoside analogue first synthesized by Sidwell et al. in 1972 [28]. It is phosphorylated by cellular adenosine kinases into ribavirin monophosphate, diphosphate, and triphosphate (RMP, RDP, and RTP, respectively) [29,30]. Ribavirin inhibits various RNA-dependent RNA polymerases such as those from influenza virus [31], vesicular stomatitis virus [32], La Crosse virus [33], Hantaan virus [34], Foot and mouth disease virus [35], West Nile virus [36], Andes virus [37], and Hepatitis C virus [38]. In contrast, ribavirin does not inhibit cellular RNA polymerase I, RNA polymerase II, and poly (A) polymerase [39]. Ribavirin inhibits the inosine monophosphate dehydrogenase, so that the *de novo* synthesis of purine nucleosides is interrupted [40]. Further, it

* Corresponding author. Address: Department of Infection Biology, Faculty of Medicine, University of Tsukuba, 1-1-1 Tennodai, Tsukuba 305-8575, Japan. Fax: +81 29 853 3233.
E-mail address: knagata@md.tsukuba.ac.jp (K. Nagata).

0006-291X/$ - see front matter © 2013 Elsevier Inc. All rights reserved.
http://dx.doi.org/10.1016/j.bbrc.2013.12.071

is proposed that ribavirin inhibits the RNA capping and RNA polymerization by virus-encoded enzymes [40]. It is also known that since ribavirin forms hydrogen bonds with cytidine and uridine, the incorporation of ribavirin into viral genomic RNA induces G to A transition leading to the lethal mutations [29].

In this study, to elucidate functional residues required for the PB1 activity, we tried to isolate PB1 mutants which are resistant to ribavirin. We found that the amino acid position 27 of PB1 is important for nucleotide recognition.

2. Materials and methods

2.1. Biological materials

Monolayer cultures of 293T and MDCK cells were maintained at 37 °C in Dulbecco's Modified Eagle Medium (DMEM) and minimal essential medium (MEM) (Nissui), respectively, supplemented with 10% fetal bovine serum (Bovogen). Influenza virus strain A/WSN/33 was prepared as previously described [8]. Ribavirin (Sigma) was dissolved in water to make stock of 100 μM.

2.2. PB1 random mutagenesis

For construction of a mammalian expression vector for PB1 containing random mutations, we used a PCR-based cloning strategy in the presence of $MnCl_2$. cDNA corresponding to the full-length PB1 was amplified with specific primers 5′-CCCCAAGCTTGCCGCC ACCATGGATGTCAATCCGACCTT-3′ and 5′-CATGCGGCCGCCTATTT TTGCCGTCTGAGCTCTT-3′. The PCR product was then cloned into the *Hind* III and *Not* I sites of pEGFP-N1 and replaced *EGFP* gene with mutated *PB1* cDNA. The mutation rate of the plasmid library was confirmed by sequencing randomly selected 20 clones using specific primer 5′-GGAAGGCTCATAGACTTCCTTA-3′, which is corresponding to the nucleotide position from 560 to 1050 of segment 2. The plasmid library was then used to analyze the influenza virus RNA polymerase activity in a mini-replicon assay system.

2.3. Mini-replicon assay system

293T cells were transfected with plasmids for the expression of viral proteins, PB1 (wild-type or mutants), PB2, PA, and NP, and a plasmid for the expression of artificial influenza virus genome containing either *EGFP* gene (for screening) or the *firely luciferase* gene (for luciferase assay) of negative polarity, which is synthesized in cells by the human DNA-dependent RNA polymerase I [41]. The mRNAs encoding either *EGFP* or *luciferase* genes are transcribed in a viral RNA polymerase-dependent manner. For the screening, ribavirin was added (0 or 75 μM) after 3 h post transfection (hpt), and the fluorescence of EGFP was observed at 15 hpt. For the luciferase assay, ribavirin was added in the medium at various concentrations after 3 hpt, incubated at 37 °C for 15 h, and then the luciferase activity was determined using commercially available reagents (Promega) according to the manufacturer's protocol. The relative luminescence intensity was measured with a luminometer for 20 s. A plasmid for the expression of *Renilla* luciferase driven by the simian virus 40 (SV40) promoter was used as an internal control for the dual-luciferase assay. As a negative control, 293T cells were transfected with the same plasmids, except for the PB1 expression plasmid.

3. Results

3.1. Screening of ribavirin-resistant PB1 mutants

To determine the 50% inhibitory concentration (IC_{50}) of ribavirin, we carried out plaque assays with WSN-infected MDCK cells in the presence of various concentrations of ribavirin (Fig. 1A). Based on the results, we determined that IC_{50} and IC_{90} of ribavirin on influenza virus were 20 and 75 μM, respectively.

To make mutated cDNA library of PB1, random mutagenesis was carried out by PCR in the presence of 0.1 mM of Mn^{2+} and 1.5 mM of Mg^{2+} as described in Section 2. To know the mutation frequency of this library, we transformed the library into *Escherichia coli* DH5α high competent cells and obtained 3×10^4 colonies. To evaluate the mutation frequency, plasmids were isolated from 20 independent colonies and sequenced between the nucleotide positions 560 and 1055 of *PB1* gene. The results of sequencing showed that approximately 4.7 mutations were introduced in 2,274 nucleotides of *PB1* gene on average (approximately 1–2 a.a./PB1 protein). Based on this in hand, we started screening of ribavirin-resistant PB1 from the mutated cDNA library as shown in Fig. 1B. At first, this library was divided into 10 groups (Group 1–10), and mini-replicon assays were performed in the presence of ribavirin at IC_{90} (Fig. 1C), and thereby EGFP-positive cells were hardly found in wild-type PB1 transfected cells. In contrast, in the case of cDNA library-transfected cells, approximately 10–30% of EGFP-positive cells were found. Among them, 34% of one of groups, Group 4-transfected cells were resistant to ribavirin on average. Thus, Group 4 was further divided into additional 10 groups and subjected to the mini-replicon assays. After enrichment by 5 time-repetitions of this cycle, we could isolate a single clone showing the resistance to ribavirin. Even in the presence of IC_{90} of ribavirin, 69% of the isolated clone-transfected cells were EGFP positive (Fig. 2A). By sequencing of the isolated clone, we found one nucleotide substitution from G to A at nucleotide position of 103 (where the 5′ terminal nucleotide of cRNA is referred to as nucleotide position 1). This nucleotide change leads to an amino acid change from Asp to Asn at amino acid position 27 (Fig. 2B).

3.2. Characterization of D27N mutant

To quantitatively measure the influenza virus RNA polymerase activity, the mini-replicon assays with the artificial genome containing *luciferase* gene was carried out in the presence of 12.5, 25, and 50 μM of ribavirin, respectively. The luciferase activity of D27N mutant remained even in the presence of ribavirin compared with that of wild type. IC_{50} of D27N to ribavirin was about 18 μM, while that of wild-type was around 10 μM (Fig. 2C). Furthermore, the expression level of D27N was confirmed by Western blot analysis. The expression level of D27N was unchanged compared with that of wild-type even in the absence or presence of 50 μM ribavirin (Fig. 2D).

To further characterize this mutant, we used methotrexate (MTX). MTX is an inhibitor for purine biosynthesis, resulting in decrease of intracellular purine concentration. The mini-replicon assays were performed in the presence of various concentrations of MTX. The viral polymerase activity of D27N was significantly more than that of wild-type even in the presence of MTX (Fig. 3).

4. Discussion

PB1 functions as a catalytic subunit of viral RNA polymerase [2–7] and contains the highly conserved motifs of RNA-dependent RNA polymerases [2]. Putative nucleotide-binding sites have been expected adjacent to the conserved motifs of RNA-dependent RNA polymerases [23,24]. PB1 also binds to the vRNA and cRNA promoters [25,27]. In this study, to elucidate the functional domain of PB1 involved in nucleotide recognition, we isolated ribavirin-resistant mutants. Ribavirin inhibits the *de novo* synthesis of purine nucleosides and thus blocks viral RNA synthesis. In addition, it has been proposed that ribavirin also inhibits directly the

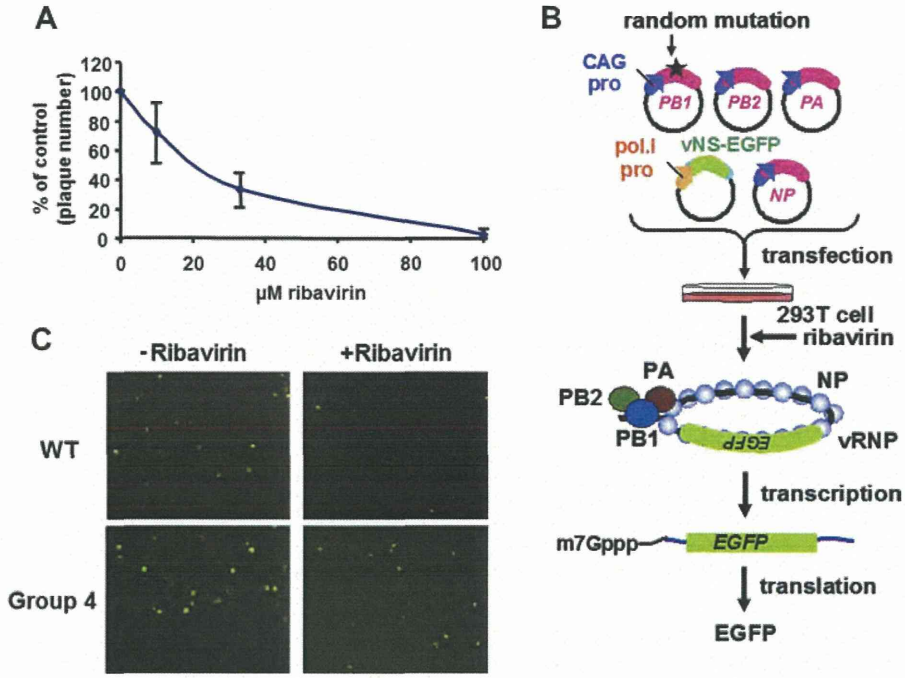

Fig. 1. Screening of ribavirin-resistant PB1 mutant. (A) Plaque assays were carried out with MDCK cells-infected WSN at MOI of 0.25×10^{-4} in the presence of ribavirin (0, 10, 33, 100, and 300 μM). The results are averages from three independent experiments with standard deviations. (B) Assay system for screening by mini-replicon assay. 293T cells were transfected with plasmids for the expression of viral proteins, PB1 (wild-type or mutant), PB2, PA, and NP, and a plasmid for the expression of artificial influenza virus genome containing *EGFP* gene of negative polarity. (C) At 3 hpt, ribavirin was added (0 or 75 μM), and the fluorescence of EGFP was observed at 15 hpt.

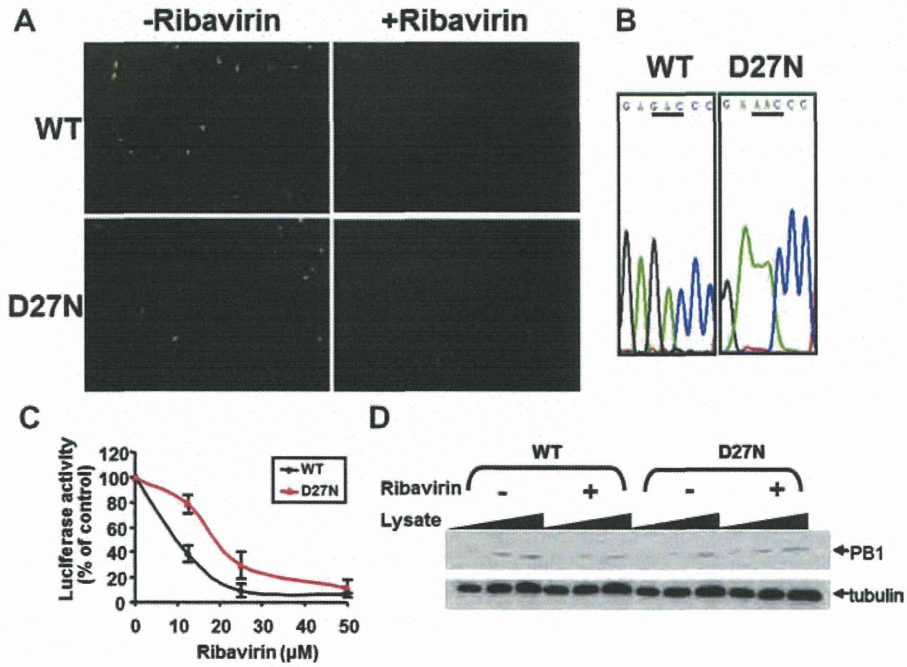

Fig. 2. Ribavirin-resistance of D27N mutant by mini-replicon assay system. (A) Mini-replicon assay using *EGFP* gene as a reporter gene. At 3 hpt, ribavirin was added (0 or 75 μM), and the fluorescence of EGFP was observed at 15 hpt. (B) Sequence of ribavirin-resistant PB1 mutant. (C) Mini-replicon assay using *luciferase* gene as a reporter gene was carried out. At 3 hpt, different concentrations (0, 12.5, 25, 50, and 100 μM) of ribavirin were added, and the luciferase activity was measured at 15 hpt. The vertical axis represents the percentage of the luciferase activity from ribavirin-treated cells relative to that from ribavirin-untreated cells. The results are averages from three independent experiments with standard deviations. (D) Effect of D27N mutation on assembly of PB1 subunit. Mini-replicon assay using *luciferase* gene as a reporter gene was carried out. At 3 hpt, ribavirin was added (0 or 50 μM). At 15 hpt, cells were lysed, and the lysates were subjected to Western blot analysis using anti-PB1 antibody and antibody against β-tubulin.